Supporting information

Flexible composite phase change materials with enhanced thermal conductivity and mechanical performance for thermal management

Shuang-Zhu Li[a], Yi-Cun Zhou[a], Lu-Ning Wang[a], Shuai-Peng Wang[a], Lu Bai[a], Chang-Ping Feng[b], Rui-Ying Bao[a], Jie Yang[a,], Ming-Bo Yang[a], Wei Yang[a,]**

[a]College of Polymer Science and Engineering, Sichuan University, State Key Laboratory of Polymer Materials Engineering, Chengdu, Sichuan, 610065 P. R. China

[b]Shandong Engineering Research Center for Additive Manufacturing, Qingdao University of Technology, Qingdao, Shandong, 266520 P. R. China

* Corresponding authors.

Tel.: + 86 28 8546 0130; fax: + 86 28 8546 0130.

Email addresses: psejieyang@scu.edu.cn (J. Yang); weiyang@scu.edu.cn (W. Yang)

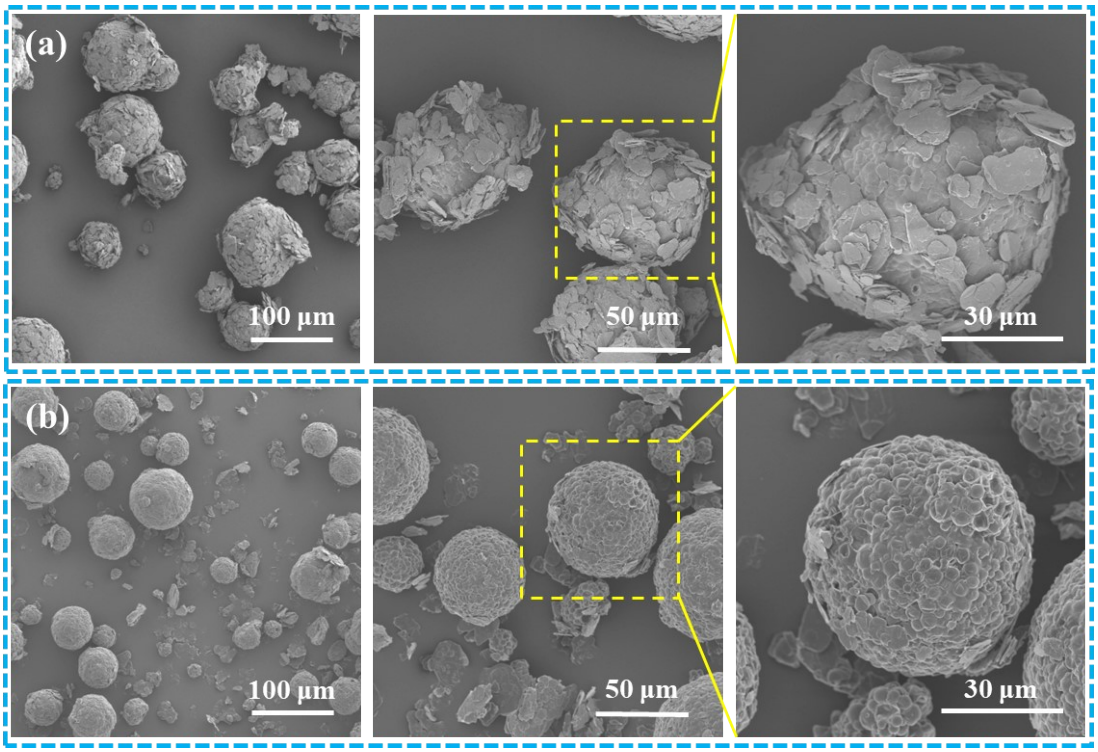

Fig. S1 SEM images of B40@M (a) with and (b) without adhesive polymers.

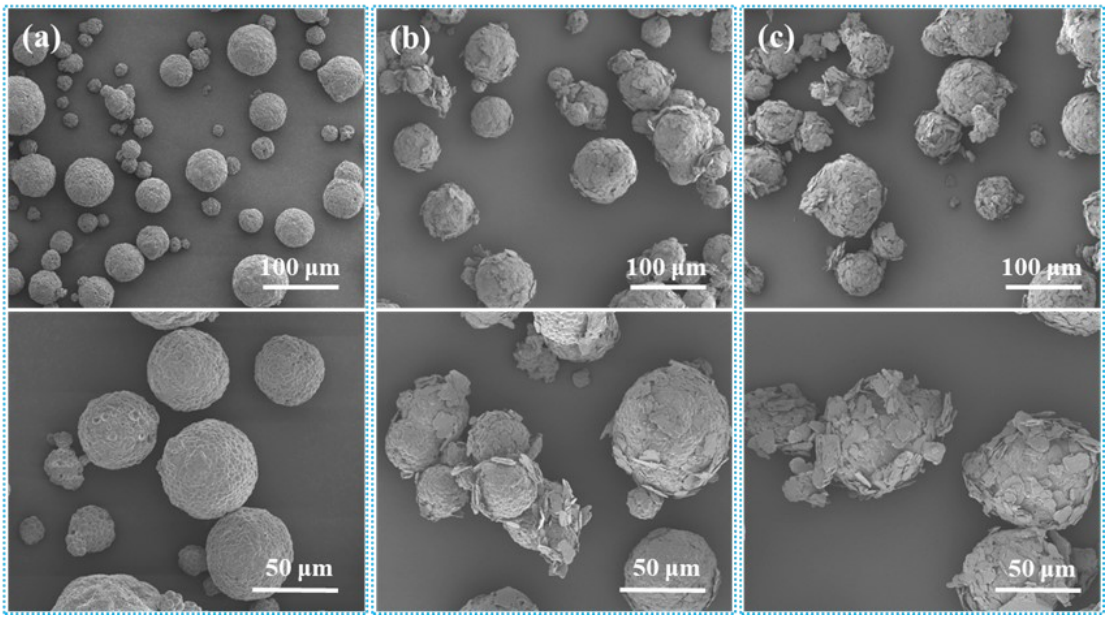

Fig. S2 SEM images of large amounts of (a) MCPW, (B)B20@M, and (c) B40@M.

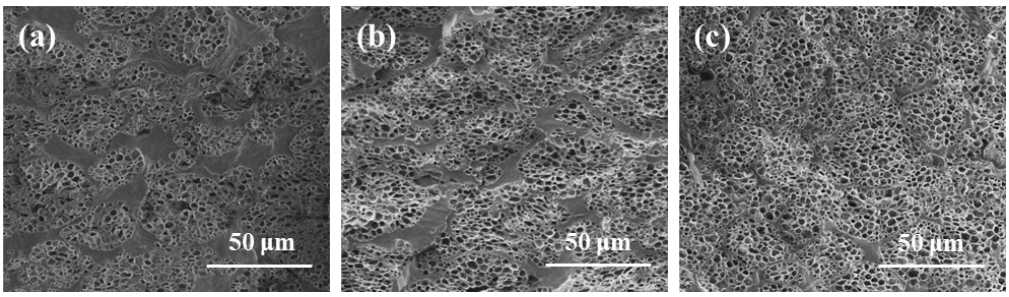

Fig. S3 Cross-sectional SEM images of (a) NM60, (b) NM70, and (c) NM80.

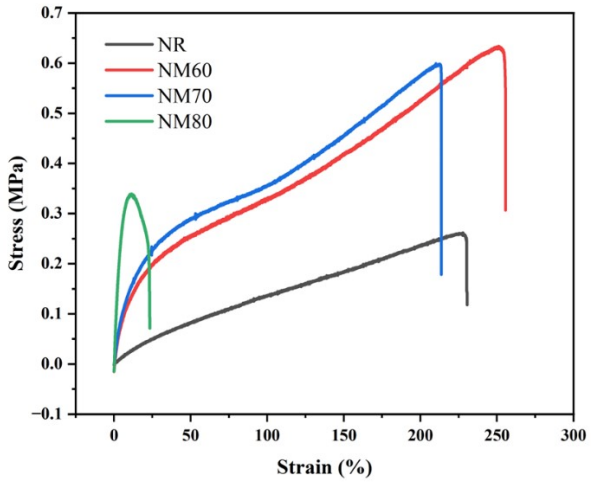

Fig. S4 Typical stress-strain curves of NR, NM60, NM70, and NM80.

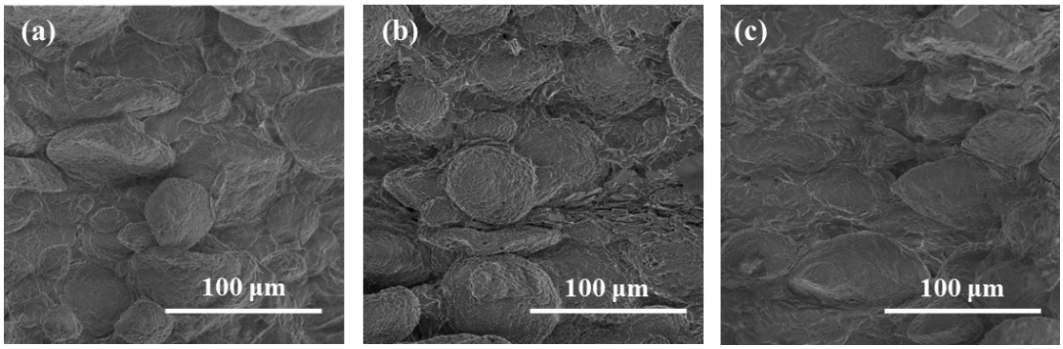

Fig. S5 Tensile fracture-surface SEM images of (a) NM70, (B)NB20/M, and (c) NB20@M.

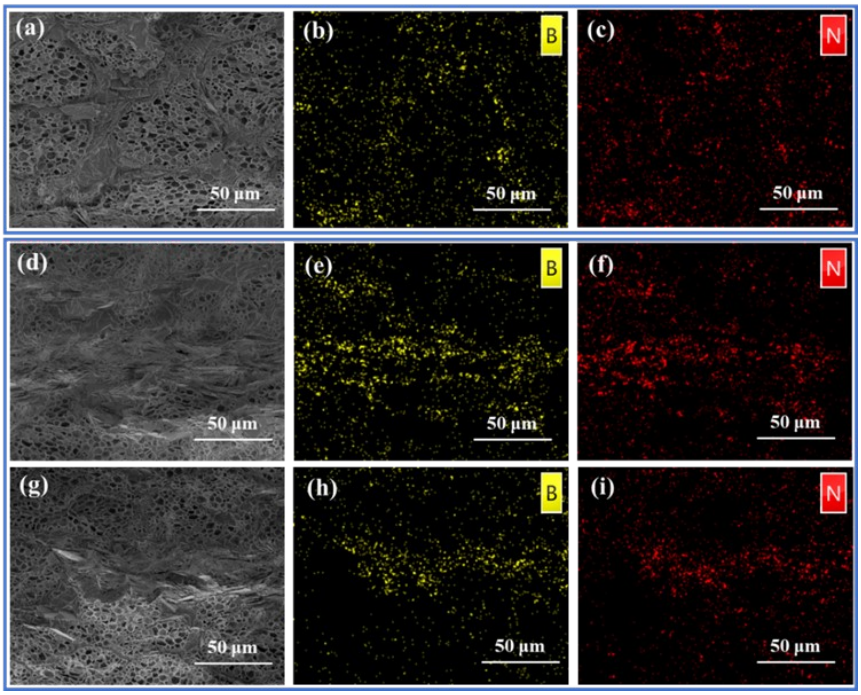

Fig. S6 Cross-sectional SEM images and corresponding mapping images of (a-c) NB20@M and (d-i) NB20/M.

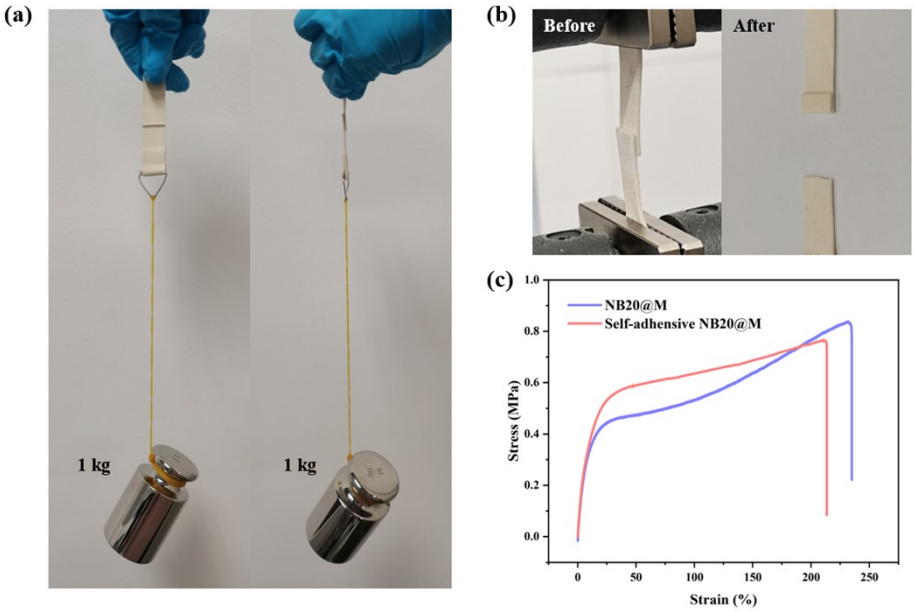

Fig. S7 Self-adhesive properties of flexible PCMs. (a) Strong self-adhesive demonstration of NB20@M: Two splines were bonded together by self-adhesion with an adhesion area of 15 × 10 mm^2. (b) Digital photos of a self-adhesive spline before and after the tensile fracture. (c) Stress-strain curves of original and self-adhesive NB20@M samples.

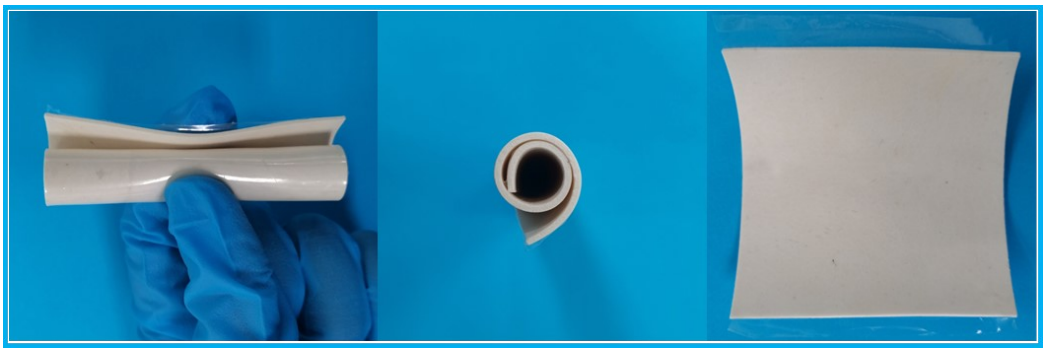

Fig. S8 Digital photos of NB20@M using as the phase change tape.

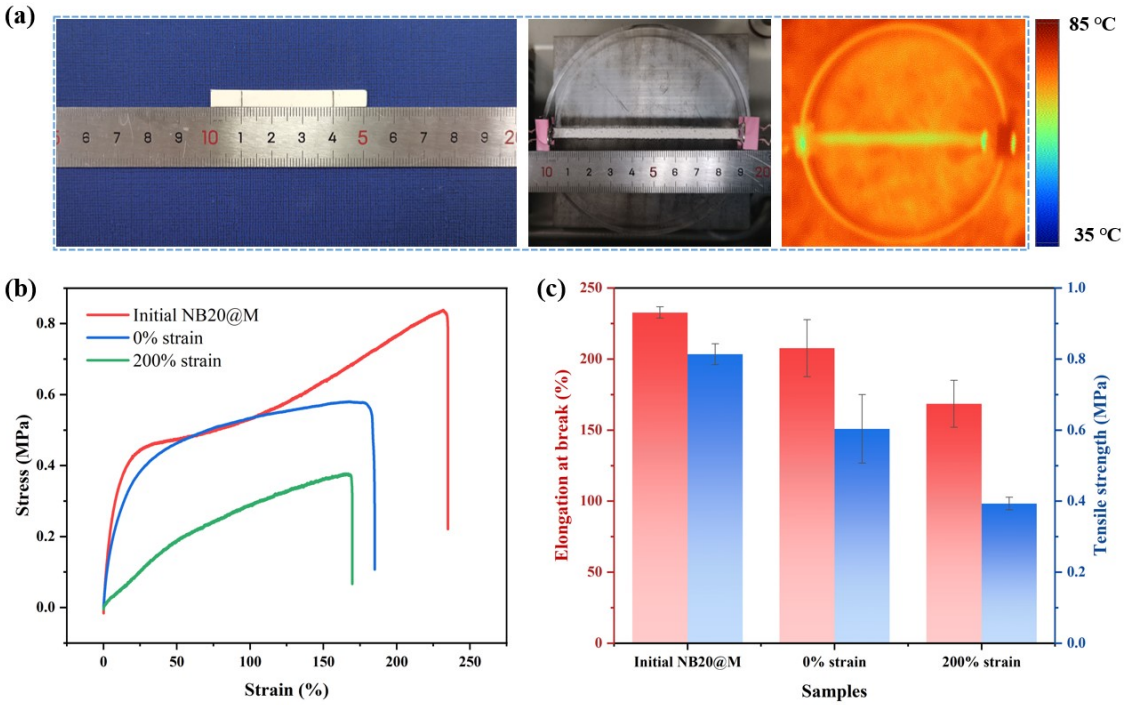

Fig. S9 (a) Digital and infrared images showing the underwater stretchability of NB20@M at 80 °C. (b) Typical stress-strain curves and (c) statistical elongational at break and tensile strength of NB20@M after the immersion and stretching in 80 °C for 24 h.

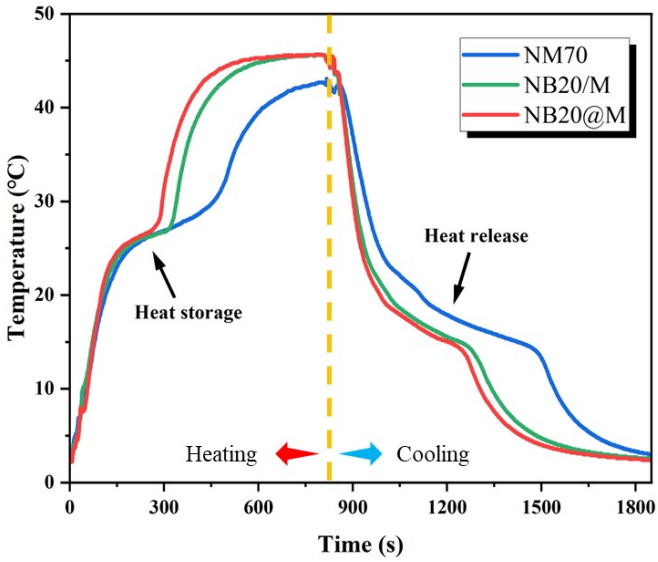

Fig. S10 Temperature evolution curves of NM70, NB20/M, and NB20@M during heating on a 50 °C hot stage and cooling on a 0 °C iron block.

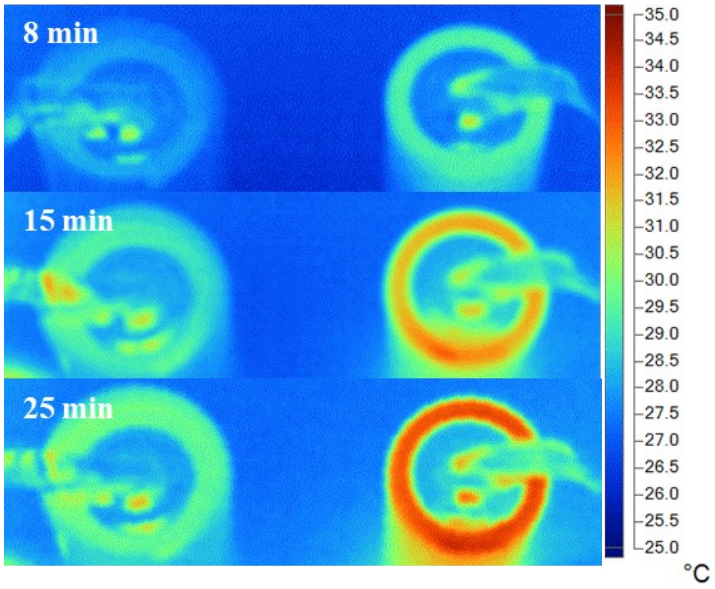

Fig. S11 Infrared images of the battery with/without NB20@M during the discharging.

Table S1 Comparison of key properties between NB20@M in this work and previously reported flexible organic PCMs.

Samples	Thermal conductivity ($W\ m^{-1}\ K^{-1}$)	Elongation at break (%)	References
OBC/PW/EG	4.2	5.4	2020[S1]
PU/CNT	0.5	6	2020[S2]
POE-SEBS/PW/BN	0.32	44	2021[S3]
POE/PW/GNP	0.73	18.75	2021[S4]
TPE/PW/EG	2.2	20	2021[S5]
EVA/EG/PA	1.7	3.68	2021[S6]
SBS/PW/CNT	0.39	20.33	2022[S7]
SEPS/n-Docosane/MWCNT/BN	0.43	101	2022[S8]
SEBS/PA/BN/Ag@HGMs	1.54	160	2022[S9]
BN@Fe_3O_4/PEG/PAA	1.07	10.4	2022[S10]
PEG/PVA/CNTs	0.065	262	2022[S11]
NB20@M	0.585	233	This work

Table S2 DSC heating and cooling characteristics of MCPW and composite PCMs.

Samples*	T_c (℃)	ΔH_c ($J\ g^{-1}$)	T_m (℃)	ΔH_m ($J\ g^{-1}$)
MCPW	11.9	192.2	30.1	193.4
NM70	8.2	128.4	33.4	129.5
NB20/M	9.3	82.6	32.2	85.3
NB20@M	8.9	83.7	32.4	86.5

*T_c, ΔH_c, T_m, and ΔH_m represent crystallization temperature, crystallization enthalpy, melting temperature, and melting enthalpy, respectively.

References

S1. S. Wu, T. Li, M. Wu, J. Xu, Y. Hu, J. Chao, T. Yan and R. Wang, *J. Mater. Chem. A*, 2020, **8**, 20011-20020.

S2. J. Shi, W. Aftab, Z. Liang, K. Yuan, M. Maqbool, H. Jiang, F. Xiong, M. Qin, S. Gao and R. Zou, *J. Mater. Chem. A*, 2020, **8**, 20133-20140.

S3. L.-Y. Yang, C.-P. Feng, L. Bai, R.-Y. Bao, Z.-Y. Liu, M.-B. Yang and W. Yang, *Chem. Eng. J.*, 2021, **425**, 131466.

S4. F. Wei, C.-P. Feng, J. Yang, L.-Y. Yang, L. Bai, R.-Y. Bao, Z.-Y. Liu, M.-B. Yang and W. Yang, *ACS Appl. Mater. Interfaces*, 2021, **13**, 59364-59372.

S5. Z. Cai, J. Liu, Y. Zhou, L. Dai, H. Wang, C. Liao, X. Zou, Y. Chen and Y. Xu, *Sol. Energy Mater. Sol. Cells*, 2021, **219**, 110728.

S6. S. Li, X. Dong, X. Lin, D. Shao, G. Zhang, J. Deng and X. Yang, *J. Energy Storage*, 2021, **44**, 103447.

S7. D. Hu, L. Han, W. Zhou, P. Li, Y. Huang, Z. Yang and X. Jia, *Chem. Eng. J.*, 2022, **437**, 135056.

S8. Y. Ma, H. Wang, L. Zhang, X. Sheng and Y. Chen, *Compos. Part A Appl. Sci. Manuf.*, 2022, **163**, 107203.

S9. H. Zhang, S. Zhang, C. Li, Z. Shi, Q. Yang, S. Wang and C. Xiong, *J. Energy Storage*, 2022, **52**, 104836.

S10. H. Cao, Y. Li, W. Xu, J. Yang, Z. Liu, L. Bai, W. Yang and M. Yang, *ACS Appl. Mater. Interfaces*, 2022, **14**, 52411-52421.

S11. J. Wu, M. Wang, L. Dong, C. Zhu, J. Shi and H. Morikawa, *ACS Sustainable Chem. Eng.*, 2022, **10**, 7873-7882.